

Ammonia and Hydrogen Vapor Cloud Explosion Testing

(A Tale of Two Gases)

Ammonia and hydrogen represent opposite ends of the spectrum with regard to the potential blast loading resulting from an accidental vapor cloud explosion (VCE), although many in industry have expressed doubts as to whether either of these fuels actually pose a VCE hazard. Ammonia is sometimes discounted as a VCE hazard due to the perceived difficulty in igniting an ammonia-air mixture and/or because of its low laminar burning velocity. Hydrogen is sometimes discounted as a VCE hazard due to the ease with which a hydrogen-air mixture can be ignited and/or because of its buoyancy. This paper presents results from ammonia and hydrogen unconfined VCE tests.

J. Kelly Thomas

Baker Engineering and Risk Consultants, Inc.
3330 Oakwell Court, Suite 100
San Antonio, TX 78218
kthomas@BakerRisk.com

Darren R. Malik

Baker Engineering and Risk Consultants, Inc.
3330 Oakwell Court, Suite 100
San Antonio, TX 78218
dmalik@BakerRisk.com

Introduction

Ammonia and hydrogen represent opposite ends of the spectrum with regard to the potential blast loading resulting from an accidental unconfined vapor cloud explosion (VCE). The maximum laminar burning velocity (LBV) of an ammonia-air mixture is in the range of 7 to 15 cm/s [1], while that for hydrogen is approximately 312 cm/s [2]. The Baker-Strehlow-Tang (BST) VCE blast load prediction methodology [3,4] defines a “low reactivity” fuel as one with an LBV less than 40 cm/s and a “high reactivity” fuel as one with an LBV greater than 75 cm/s. Hence, the ammonia LBV is well below the maximum for a low

reactivity fuel and the hydrogen LBV is well above the minimum for a high reactivity fuel. For reference, methane and ethylene are typically taken as the “prototypical” low and high reactivity fuels, and these have LBVs of 40 cm/s and 80 cm/s, respectively [2].

There have been questions raised as to whether ammonia or hydrogen actually pose a VCE hazard. Ammonia is sometimes discounted as a VCE hazard due to the perceived difficulty in igniting a flammable ammonia-air mixture and/or because of its low LBV. While ammonia does have a relatively high minimum ignition energy (MIE) and hence may be less likely to ignite than typical hydrocarbon fuels, it can be ignited by a sufficiently strong ignition source,

as shown by the tests described in this paper. Ruling out an ammonia-air VCE based on an assumption that the mixture cannot be ignited is therefore not justified without careful consideration of potential ignition sources. However, the impression that ammonia does not pose a VCE hazard is supported by the lack of any reported accidental unconfined ammonia VCE which has produced damaging blast loads [5]. The Factory Mutual guideline for VCE evaluation expressly excludes NH₃ outdoor releases as credible VCE scenarios [6].

Hydrogen is sometimes discounted as a VCE hazard due to the ease with which a flammable hydrogen-air mixture can be ignited (i.e., its low MIE), which suggests that a hydrogen release is likely to be ignited before a flammable hydrogen-air cloud with sufficient volume to produce significant VCE blast loads can form. While the low MIE of hydrogen does indeed suggest that prompt ignition is much more likely than for typical hydrocarbon fuels, it does not imply that delayed ignition will not occur [7]. Hydrogen is also sometimes discounted as a VCE hazard due to its buoyancy, which suggests that a hydrogen release will “float away” before a flammable cloud with sufficient volume to produce significant blast loads can form. While a hydrogen-air mixture is buoyant (i.e., if the hydrogen release is not very cold), the dispersion of a high pressure hydrogen release will not be influenced by this buoyancy during the momentum dominated dispersion phase, which can result in a large flammable hydrogen-air cloud being formed at grade-level [8, 9]. Furthermore, assertions that hydrogen cannot pose a VCE hazard are contradicted by the existence of accidental unconfined hydrogen VCEs that have produced damaging blast loads [10].

This paper presents the results of VCE testing performed with both ammonia and hydrogen in congested volumes without the presence of confinement [11,12]. The tests with ammonia were performed using a worst-case concentration in a highly congested rig with a length of 72 feet, a

width of 12 feet and a height of 6 feet. The mixture was ignited against a large wall placed at one end of the rig. The tests with hydrogen were performed in a similar test rig, but with a lower level of congestion (i.e., reduced flame acceleration for a given fuel), a shorter length (48 feet), with central ignition rather than end ignition, and without the presence of an end wall. The hydrogen tests spanned a range of lean concentrations, from 16% up to 22% hydrogen (vs. a stoichiometric concentration of 30%).

Ammonia VCE Tests

Test Description

Rig Configuration

The ammonia VCE tests were carried out in a relatively long highly congested test rig in order to promote flame acceleration and the generation of measurable blast loads. Methane VCE tests were performed in the same rig to provide a basis of comparison with the ammonia VCE tests. The test rig was 72 feet (22 m) long, 12 feet (3.7 m) wide and 6 feet (1.8 m) high. A wall [26 ft. (7.9 m) wide by 16 ft. (4.9 m) high] was placed at the end of the rig where the flammable mixture was ignited. An isometric view and photograph of the test rig are provided in Figure 1. With the exception of the wall at the rig end, no confinement was present within the rig.

The same high congestion level used in the creation of the BST flame speed tables [4] was used in these tests. The array was made up of a regular array of vertical circular tubes [2.375-inch (6 cm) diameter, area and volume blockage ratios of 23% and 5.7%, respectively]. For each 6 ft (1.8 m) cube, a total of 61 vertical tubes were installed, along with the 4 cube corner supports. A plan view showing the congestion pattern is provided in Figure 2. This congestion pattern is intended to be conservative (i.e., highly congested) relative to the congestion in a typical process plant.

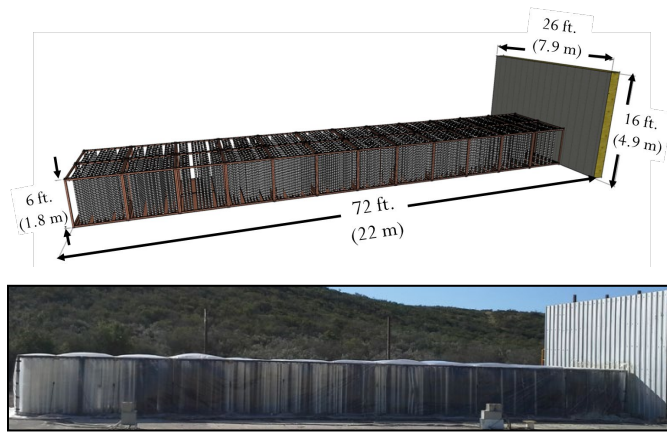


Figure 1. 3D Isometric and Photographic View of Ammonia & Methane Test Rig

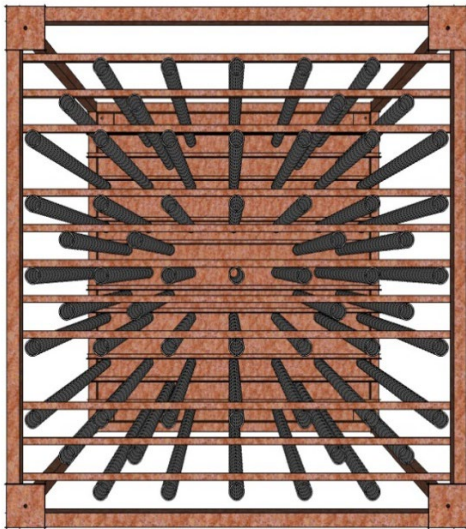


Figure 2. High Congestion Pattern Used in Ammonia & Methane Tests

Fuel-Air Mixture

The entire test rig was covered in a 1.5 mil (0.0015 in., 0.038 mm) thick plastic sheet prior to the start of the test. The sheet was retained by 12 straps placed along the length of the rig during the generation of the fuel-air mixture. A quiescent wait period was followed once the target concentration was achieved. The straps were released via remote actuators just prior to ignition in order to allow the VCE to expand as freely as possible.

Upper and lower fuel concentration acceptance bands were established to minimize the impact

of fuel concentration variations. The acceptable concentrations were based on a 1% decrease from the maximum LBV. The target fuel concentration for ammonia tests was 23.2%, with an acceptance range of 22.9% to 23.6%, based on a -1% change from the maximum LBV reported by Duynslaegher [1]. The target fuel concentration for methane tests was 10.0%, with an acceptance range of 9.9% to 10.5%.

The fuel and air were mixed and introduced into the rig through a series of venturis oriented to expel the enriched fuel-air mixture downward. The rig was divided into 3 fuel delivery zones with four venturis each zone in order to support the generation of a uniform fuel-air mixture throughout the rig. The locations of the venturis are shown in Figure 3. Each venturi was 3 feet (0.91 m) off the rig centerline at a height of 3 feet (0.91 m).

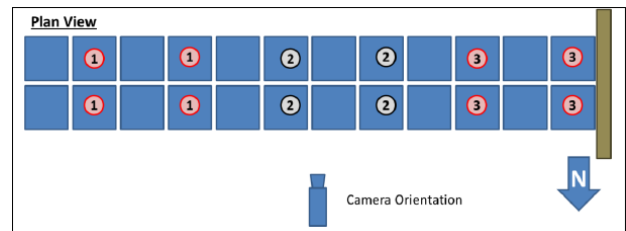


Figure 3. Fuel Delivery Venturi Locations for Ammonia and Methane Tests

Fans were used to circulate the fuel-air mixture in order to quickly achieve a uniform mixture throughout the rig. The fans were positioned at the center of each cube at a height of 5.5 ft. and oriented downward. Each fan was rated for a 110 cfm flow rate, which is equivalent to turning the rig volume over every two minutes. The fans were shut off prior to ignition in order to allow the mixture to reach a quiescent state.

Fuel concentrations were determined indirectly based on oxygen concentration. The oxygen analyzer was calibrated prior to each test using a known concentration of a suitable span gas balanced with nitrogen and with nitrogen as the zero gas. The sample points used to monitor concentration during the test were distributed along

the long axis of the rig in the pattern, as shown in Figure 4. Gas samples were pulled through 0.18-in (0.46 cm) inner diameter sample lines, ranging in length from 30 to 80 ft (9 to 24 m), depending on the sample point. The sample pump flow rate was 10 ft³/hr (17 m³/min), giving a transit time from the sample point to the analyzer of 2 to 5 seconds. The time required for the analyzer to reach 90% of full scale is 30 seconds. The combined time for a sample to reach the analyzer and for the analyzer to respond was therefore approximately one half minute. This allowed the 5 sample points to be cycled through in approximately 3 minutes.

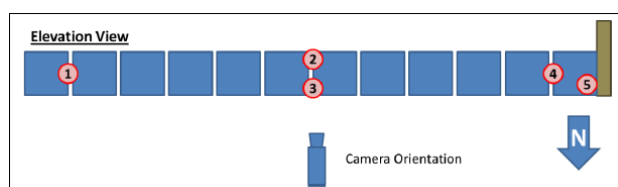


Figure 4. Fuel Sampling Locations for Ammonia and Methane Tests

Ignition Systems

The location of the ignition source was grade level along the rig centerline near the end wall. Two different ignition systems were used during the course of this test program. The first two methane tests (A01 and A02) were ignited with an exploding fuse wire. A spark gap ignition system was deployed for the last methane test (A03) and all ammonia tests (B01-B03) due to concerns about releasing a toxic cloud of ammonia if the exploding fuse wire system failed to ignite the cloud. The spark gap ignition system was safer in this regard because it could be fired continuously in the event a test needed to be aborted. Conversely, the fuse wire system could only be fired twice (primary and secondary igniters). There was no significant difference in the methane test results due to the ignition system change.

The fuse wire was 5 cm long and had a nominal ignition energy of 50 J (9.6 J/cm heat of combustion). The spark gap ignition system was composed of a 15 kV transformer with two steel

electrodes separated by a nominal 0.25 inch (0.64 cm) air gap.

Instrumentation

Blast pressure histories were measured using PCB® Piezotronics general purpose ICP® dynamic pressure sensors (Model CA102B18) connected to a line-powered ICP® sensor signal conditioner using microdot connectors and BNC cables. Each pressure gauge was mounted on a ½-inch steel plate approximately 12 inches (30 cm) in length and width. The pressure gauges internal to the test rig were installed with the pressure gauge mounted in a recess to reduce the effects of thermal radiation from the fireball. The gauges external to the rig were installed with the face of the gauge flush with the top of the mount. The signal from each pressure sensor was recorded using a National Instruments PXIE-1082 Chassis. A schematic of the pressure transducer array is shown in Figure 5; the farthest gauge along a gauge line is at roughly 300 feet from the ignition location.

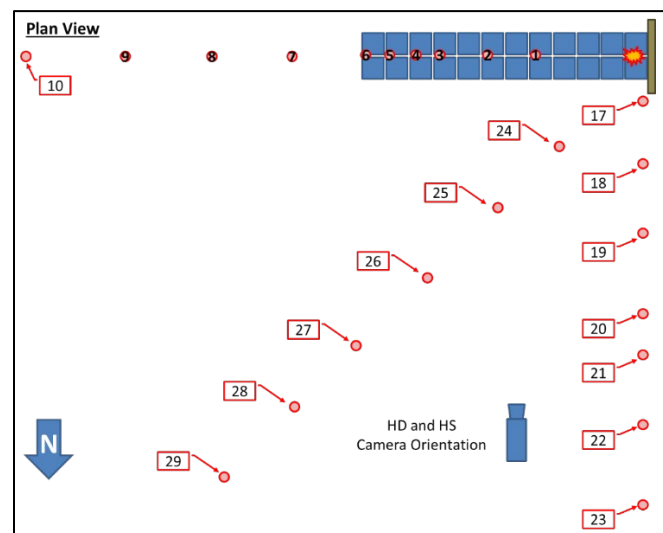


Figure 5. Schematic of the Pressure Transducer Array and Video Cameras

Flame propagation was observed with regular speed high definition and high speed video. The locations of the high speed and high definition cameras are shown in Figure 5. The high-speed camera was set to record between 500 to 1000 frames per second based on the expected flame

speed. The high definition video was captured at 30 frames per second.

Results

The measured fuel concentration for each test prior to ignition is provided in Table 1. Table 2 provides a series of still frames which qualitatively shows the relative time of arrival for the flame propagation through the rig for the two fuel species. The HD camera frame rate does not provide sufficient resolution to rigorously match the time of arrival at the same discrete locations for both tests.

Table 1. Fuel Concentrations

Methane		Ammonia	
Test ID	Concentration (%)	Test ID	Concentration (%)
A01	10.0	B01	23.2
A02	10.4	B02	23.0
A03	10.5	B03	23.1

However, the still frames and approximate times provided in Table 2 provide a qualitative indication of the slow flame speed propagation observed in the ammonia tests in relation to the methane tests. The actual flame speed analysis which is reported in the following paragraphs was determined using the high speed video data.

Methane Tests

The measured peak pressures for the long axis gauge lane is Figure 6 as a function of the distance from the ignition location. The test data are shown as points in these figures. The line provided in the figures was generated using BakerRisk's SafeSite_{3G}[®] code [13] with a BST flame speed of Mach 0.19, which was the selected based on a least squares fit analysis of the test data. The location of the end of the test rig is also denoted in this figure.

The observed flame speeds are provided in Figure 7. The maximum and average flame speeds in the rig were approximately 500 ft/s (150 m/s, Mach 0.44) and 350 ft/s (110 m/s,

















Mach 0.31), respectively. The discrepancy between the observed average flame speed (Mach 0.31) and the least squares fit BST flame speed (Mach 0.19) is due to the test rig aspect ratio, the variance of the flame speed along the length of the rig, and the asymmetric flame propagation (i.e., propagating in a single direction along the rig centerline). The use of the least squares fit BST flame speed is consistent with the derivation of the flame speeds in the published BST flame speed table [4]. The BST flame speed of Mach 0.19 under predicts the measured peak pressures in the far field along the direction of flame propagation, but over predicts the measured peak pressures in the far field in the transverse direction.

Ammonia Tests

The ammonia-air tests did not produce measurable overpressures due to the low flame speed developed in these tests. A plot of the observed ammonia-air flame speeds is provided in Figure 8. The flame speeds observed in Tests B01 and B02 were higher than that observed in Test B03. A possible explanation for this difference is the wind direction.

Tests B01 and B02 were performed with a 5-10 mph (7.3-15 ft/s, 2.2-4.5 m/s) wind blowing in the direction of flame propagation, approximately 30 degrees off the long axis of the rig. Test B03 was performed with a 5 mph wind blowing perpendicular to the direction of flame travel. Correcting Test B01 and B02 for an 8 ft/s (2.4 m/s) flow field along the direction of flame propagation results in the wind corrected ammonia flame speeds shown in Figure 9. The wind adjusted flame speeds for Test B01 and Test B02 are in reasonably good agreement with Test B03. The reason for the higher flame speed in Test B01 near the end of the rig is unknown, but it is acknowledged that the derivation of flame speed from video at very low flame speeds is subject to increased uncertainty.

Table 2. Selected Still Frames Showing Relative Flame Propagation

Approximate Flame Location	Methane Test A03			Ammonia Test B01		
	Frame #	Time [s]	Still Frame	Frame #	Time [s]	Still Frame
Ignition	0	0.00		0	0.0	
2 cubes	2	0.07		30	1.0	
3 cubes	4	0.13		48	1.6	
6 cubes	5	0.17		73	2.4	
8 cubes	6	0.20		107	3.6	
10 Cubes	7	0.23		117	3.9	
12 Cubes	8	0.27		132	4.4	
End of Camera Frame	9	0.30		142	4.7	

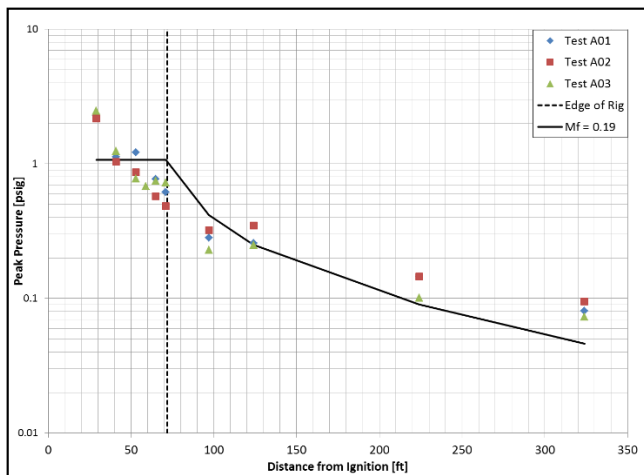


Figure 6. Measured Peak Pressures along the East (long axis) Gauge Lane (methane)

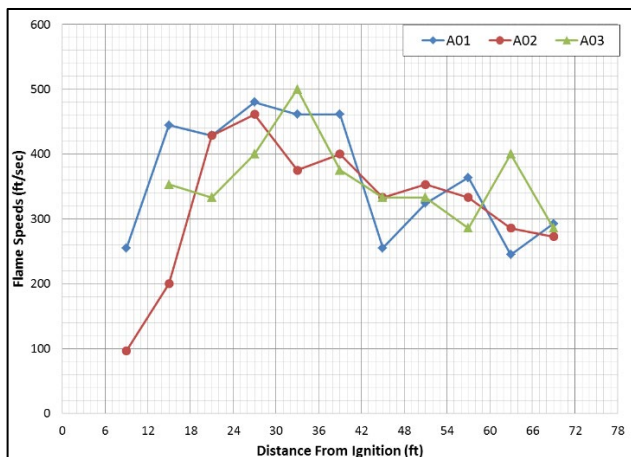


Figure 7. Observed Methane Flame Speeds

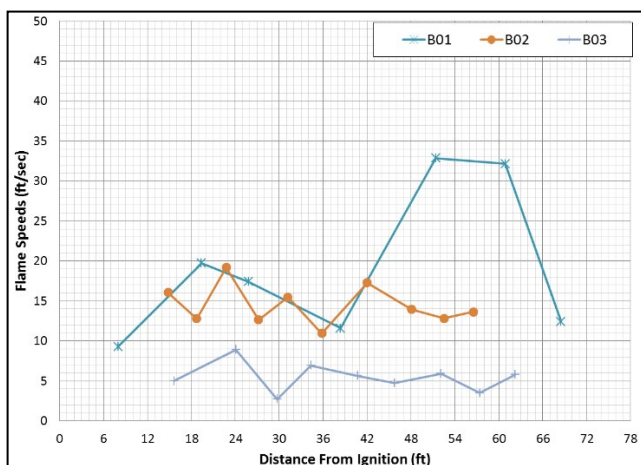


Figure 8. Observed Ammonia Flame Speeds

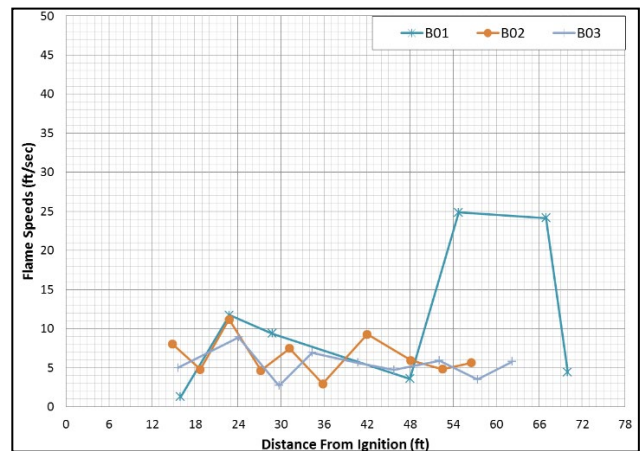


Figure 9. Wind-Corrected Ammonia Flame Speeds

Video analysis of all three ammonia test confirmed that the tent remained in place for all three ammonia tests despite the change in wind direction between Test B02 and Test B03. The relative stability of the tent ahead of the flame front can be seen in the still frames provided in Table 2.

Discussion

The methane-air VCE tests produced maximum blast pressures of approximately 2 psig (0.1 kPa) and maximum flame speeds of approximately 500 ft/s (150 m/s, Mach 0.44). The ammonia VCE tests did not produce measureable overpressures and the observed maximum flame speeds were approximately 25 ft/s (7.6 m/s, Mach 0.02), a factor of 20 lower than in the methane air tests.

An updated BST flame speed table with a new “very low” reactivity class is provided in Table 3 in order to scale the results of this test program for use in a consequence or risk-based facility siting. The values given for the “very low” reactivity fuel class in Table 3 were calculated by multiplying the low reactivity flame speeds by the ratio observed ammonia-air flame speed (Mach 0.02) and the flame speed based on the least squares fit analysis of the methane blast overpressure data (Mach 0.19); even lower values would result if the maximum observed methane flame speed (Mach 0.44) were employed.

Table 3. Updated BST Flame Speed Table with Very Low Reactivity Class

Confinement	Reactivity	Congestion		
		High	Medium	Low
2-D	High	DDT	DDT	0.59
	Medium	1.6	0.66	0.47
	Low	0.66	0.47	0.079
	Very-Low	0.069	0.049	0.008
2.5-D	High	DDT	DDT	0.47
	Medium	1	0.55	0.29
	Low	0.5	0.35	0.053
	Very-Low	0.053	0.037	0.006
3-D	High	DDT	DDT	0.36
	Medium	0.5	0.44	0.11
	Low	0.34	0.23	0.026
	Very-Low	0.036	0.024	0.003

To illustrate the VCE blast loads expected for the “very low” fuel reactivity class, consider a congested volume with a footprint of 200 ft (61 m) by 200 ft (61 m) and a height of 25 ft (7.6 m), which gives a total volume of 1.0×10^6 ft³ (28,000 m³). Even if the entire congested volume is treated as high congestion with 2-D confinement ($M_f = 0.069$), which would be a very extreme case, the blast overpressure at a standoff from the congested volume center of 150 feet based on the BST VCE blast load prediction method would only be 0.1 psig. Hence, unconfined VCEs of fuels in the “very low” reactivity class (e.g., ammonia) do not appear capable of causing damaging blast loads, even under relatively severe conditions. Similar conclusions are drawn from applying the GAMES correlation [14].

Hydrogen VCE Tests

Test Description

The test rig for the hydrogen VCE tests was the same as had been previously used by BakerRisk for ethylene VCE testing [15,16]. The rig is similar to that described for the ammonia tests, but the rig was shorter [48 feet (14.6 m)], less congested and did not utilize an end wall. The congestion arrangement was made up of vertical circular tubes [2.375-inch (6 cm) diameter] giving a pitch-to-diameter ratio of 4.5 and provides area and volume blockage ratios of 22% and

4.1%, respectively. For each 6 ft (1.8 m) cube, a total of 45 vertical tubes were installed, along with the 4 cube corner supports. This level of congestion corresponds to the “medium” congestion level in the BST flame speed table [4]. An illustration and photograph of the test rig in this configuration are shown in Figure 10 and Figure 11, respectively. The test rig was configured without any confinement (i.e., no wall or roof sections).

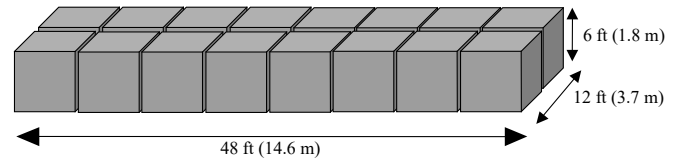


Figure 10. Schematic of Hydrogen Test Rig



Figure 11. Photograph of Hydrogen Test Rig

The hydrogen-air mixtures were developed in essentially the same way as described for the ammonia VCE tests. Six venturis deployed down the length of the rig (mid height) and directed downward were employed to inject the fuel, with additional mixing provided by 16 fans mounted at the top of the rig (1 per cube). The mixture was sampled from 4 different points in the rig to confirm that a uniform mixture at the desired concentration prior to ignition. The fuel was injected over a period of one-half to one hour, and a quiescent period of 5 to 20 minutes was observed prior to ignition. The target hydrogen concentrations for these tests were 16%, 18%, 20% and 22%; all of these mixtures are lean (i.e., stoichiometric concentration is 30%).

The mixture was ignited at the center of the rig near grade level using an electrochemical match. The instrumentation used in these tests was essentially the same as for the ammonia tests (i.e.,

normal speed video, high speed video and dynamic pressure sensors).

Results

The measured fuel concentration for each test prior to ignition is provided in Table 4.

Table 4. Hydrogen Fuel Concentrations

Test ID	Concentration (%)
H01	16.0
H02	18.1
H04	20.1
H05	22.2

The pressure histories for monitor point locations external to the rig for Test H02 (18% H₂), Test H04 (20% H₂) and Test H05 (22% H₂) are shown in Figure 12, Figure 13 and Figure 14, respectively. The pressure histories for these three tests at a location 8 feet outside the rig along the long axis are compared in Figure 15. Figure 16 shows the peak blast overpressure as a function of the distance from the ignition location (i.e., rig center). The peak pressures measured within the test rig for all 4 hydrogen tests are summarized in Table 5.

Discussion

High speed video analysis showed that a deflagration-to-detonation transition (DDT) occurred in Test H05 (22% H₂) near the end of the rig, with a detonation wave traveling at approximately Mach 5 traversing the remainder of the hydrogen-air mixture. This is consistent with peak pressures above 100 psig being measured in the test. Conversely, a DDT was not observed in Test H04 (20% H₂), although the blast loads were still high (34 psig maximum within the rig) and a flame speed of approximately Mach 1 was reached.

These test clearly demonstrated that an H₂-air mixture, if allowed to accumulate and ignite, can provide a significant VCE. In the presence of moderate congestion, even with no confinement, lean hydrogen mixtures can undergo a DDT.

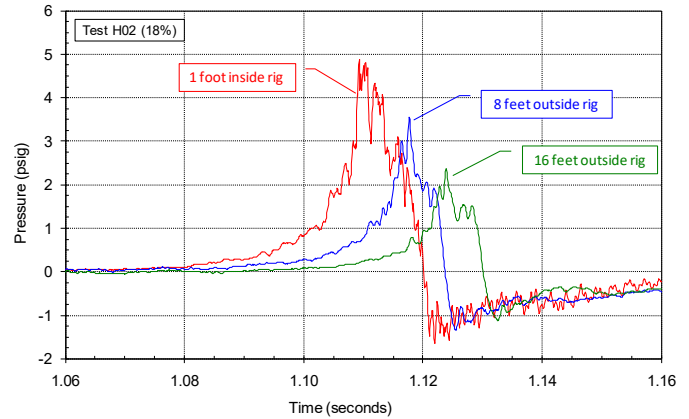


Figure 12. Selected Pressure Histories for Hydrogen Test H02 (18% H₂)

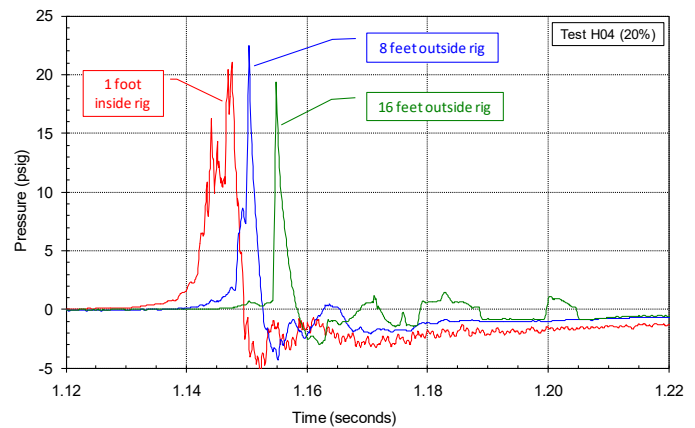


Figure 13. Selected Pressure Histories for Hydrogen Test H04 (20% H₂)

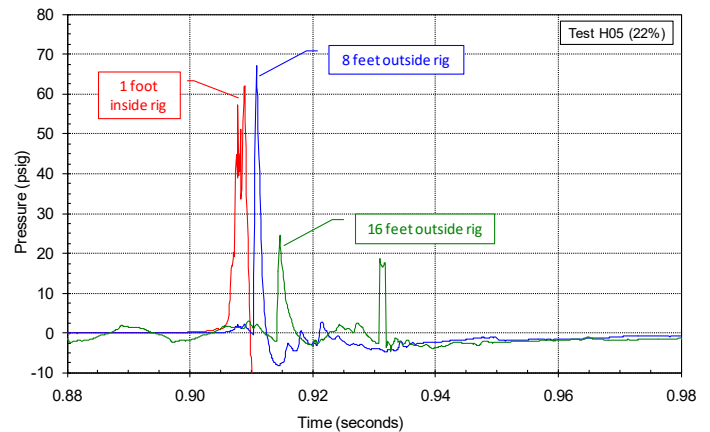


Figure 14. Selected Pressure Histories for Hydrogen Test H05 (22% H₂)

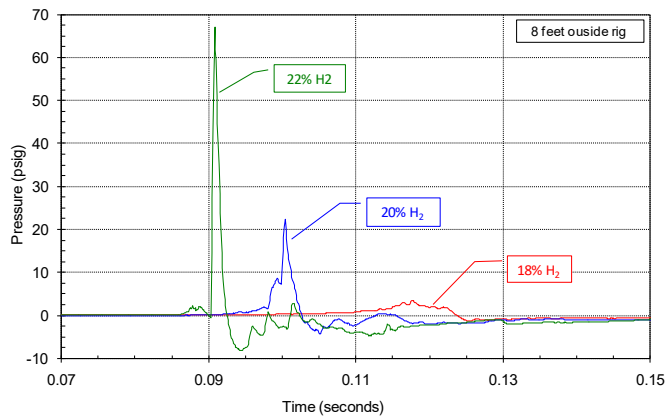


Figure 15. Pressure Histories at 8 Feet Outside Rig (hydrogen)

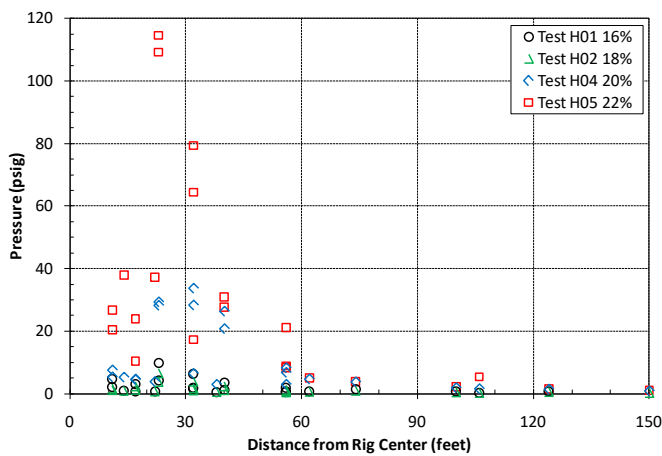


Figure 16. Measured Peak Pressures along Long Gauge Lane (hydrogen)

Table 5. Peak Pressures for Hydrogen Tests

Test ID	Concentration (%)	Equivalence Ratio	Peak Pressure (psig)
H01	16.0	0.44	9.9
H02	18.1	0.51	6.6
H04	20.1	0.58	34
H05	22.2	0.66	115

Conclusions

The ammonia VCE tests described in this paper clearly demonstrate that damaging blast loads for unconfined ammonia VCEs would not be expected due to the very low LBV of ammonia and

the resultant low VCE flame speeds. This is consistent with expectations [5,6]. A “very low” BST flame speed was developed based on these tests. Example blast load calculations show that, even for a relatively severe VCE, damaging blast loads external to the congested volume in which an ammonia-air cloud accumulates would not be expected. It is important to note that the results of the ammonia VCE tests are only applicable to unconfined VCE scenarios. Confined scenarios (i.e., indoor explosions) would behave differently. Testing of confined VCEs with very low reactivity fuels (e.g., ammonia) would be required to define the corresponding explosion hazard, as well as the level of conservatism in the current blast load prediction methodologies for such scenarios. Given the potential for internal vapor cloud explosions to create damaging overpressures, a logical next step would be to perform such tests to better define the explosion hazard associated with such very low reactivity fuels.

The hydrogen VCE tests described in this paper clearly demonstrate that even lean hydrogen-air mixtures can undergo a DDT and medium congestion levels even in the absence of confinement. This result was expected based on prior VCE testing performed in the same test rig using ethylene. It should be noted that a detonation, once triggered by a DDT, can propagate through essentially all the flammable cloud, including that outside the congested volume, which can dramatically increase the VCE blast load relative to that for a deflagration [16]. The potential for a DDT should therefore be considered for release scenarios involving high reactivity fuels (e.g., hydrogen, ethylene, etc.). The data from these tests were used, along with data from the ethylene tests performed by BakerRisk and other data in the literature, to develop DDT evaluation criteria [17]. These criteria can be utilized to evaluate the potential for a DDT in actual plant geometries.

Acknowledgements

The ammonia and methane tests were performed under the sponsorship of Honeywell International, Inc., and their support is gratefully acknowledged. Brad Horn, Jef Rowley, Martin Goodrich, Austin Burch and Emeka Ugwu were instrumental in the completion of these tests and their contribution to this work is also gratefully acknowledged. The hydrogen tests were performed as a BakerRisk Internal Research program; the support of Martin Goodrich and Robert Duran in performing these tests is gratefully acknowledged.

-
- [1] Duynslaegher, Catherine (2011) "Experimental and Numerical Study of Ammonia Combustion" Université catholique de Louvain. Sept. 2011.
 - [2] National Fire Protection Association (2007) Standard on Explosion Protection by Deflagration Venting (NFPA 68), Quincy, MA.
 - [3] Baker, Q.A. et al. (2010) Guidelines for Vapor Cloud Explosion, Pressure Vessel Burst, BLEVE and Flash Fire Hazards, 2nd Edition, AIChE CCPS & John Wiley and Sons, New York, NY.
 - [4] Pierorazio, A.J., J.K. Thomas, Q.A. Baker and D.E. Ketchum (2005) "An Update to the Baker-Strehlow Tang Vapor Cloud Explosion Prediction Methodology Flame Speed Table," Process Safety Progress, 24(1): 59-65.
 - [5] Baker, Q.A., K.A. Dejmek and X. Qin (2008) "Facility Siting in Ammonia Facilities," AIChE 53rd Annual Safety in Ammonia Plants and Related Facilities Symp., Paper 3e, San Antonio, TX, Sept. 9, 2008.
 - [6] Factory Mutual Global, Property Loss Prevention Data Sheets, 7-42, "Guidelines for Evaluating the Effect of Vapor Cloud Explosions Using a Flame Acceleration Method," Oct. 2008.
 - [7] Moosemiller, M. and B. Galindo, "Hydrogen Ignitions – Wildly Differing Opinions, and Why Everyone Could be Right," 10th Global Congress on Process Safety, AIChE Annual Mtg, New Orleans, LA, Mar 30 – Apr 2, 2014.
 - [8] Miller, D., C.D. Eastwood and J.K. Thomas (2015) "Hydrogen Jet Vapor Cloud Explosion: Test Data and Comparison with Predictions," AIChE 11th Global Congress on Process Safety (49th Loss Prevention Symposium), Austin, TX, April 26-30, 2015.
 - [9] Jallais, S., E. Vyazmina, D. Miller and J.K. Thomas (2017) "Hydrogen Jet Vapor Cloud Explosion: A Model for Predicting Blast Size and Application to Risk Assessment," AIChE 13th Global Congress on Process Safety (51st Loss Prevention Symposium), San Antonio, TX, March 26-29, 2017.
 - [10] Thomas, J.K., C.D. Eastwood and M.L. Goodrich (2015) "Are Unconfined Hydrogen Vapor Cloud Explosions Credible?" Process Safety Progress, 34(1): 36-43 (presented at AIChE 10th Global Congress on Process Safety / 48th Loss Prevention Symposium, New Orleans, LA, Mar 30-Apr 2, 2014).
 - [11] Downes, A.M., S. Rogers, D.R. Malik and J.K. Thomas (2016) "Ammonia VCE Testing and Implications for FSS Consequence Analyses and Risk Assessments," AIChE 12th Global Congress on Process Safety (50th Loss Prevention Symposium), Houston, TX, April 11-13, 2016.
 - [12] Thomas, J.K., R.J. Duran and M.L. Goodrich (2010) "Deflagration to Detonation Transition in a Lean Hydrogen-Air Unconfined Vapor Cloud Explosion," Mary Kay O'Connor Process Safety International Symposium, College Station, TX, October 27, 2010.
 - [13] Version 2012.1.31 Release Date: Aug. 30 2014, DLL Aug. 30 2014.
 - [14] Mercx, W.P.M., A.C. van den Berg. And D. van Leeuwen (1998) Application of Correlations to Quantify the Source Strength of Vapour Cloud Explosions in Realistic Situations, Final Report for the project: 'GAMES', TNO Prins Maurits Laboratory.
 - [15] Thomas, J.K., A.J. Pierorazio, M. Goodrich, M. Kolbe, Q.A. Baker and D.E. Ketchum (2003) "Deflagration to Detonation Transition in Unconfined Vapor Cloud Explosions," Center for Chemical Process Safety (CCPS) 18th Annual International Conference & Workshop, Scottsdale, AZ, 23-25 September 2003.
 - [16] Thomas, J.K., M.L. Goodrich and R.J. Duran (2013) "Propagation of a Vapor Cloud Detonation from a Congested Area into an Uncongested Area: Demonstration Test and Impact on Blast Load Prediction," Process Safety Progress, 32(2): 199-206 (presented at AIChE 8th Global Congress on Process Safety / 46th Loss Prevention Symposium, Houston, TX, April 1-5, 2012).
 - [17] Thomas, J.K., J. Geng and C.D. Eastwood (2011) "Comparison of Deflagration to Detonation Transition (DDT) Criteria for With Test Data from Unconfined Ethylene-Air Vapor Cloud Explosion," AIChE 7th Global Congress on Process Safety (45th Annual Loss Prevention Symp.), Chicago, IL, March 13-16, 2011.